Alluvial soils as paleoenvironmental indicator in fluvial environments: a case study from Colombia

Juan Carlos Loaiza-Usuga*, María Isabel Toro-Quijano, Marion Weber-Scharff

Universidad Nacional de Colombia, Sede Medellín, Facultad de Minas, Departamento de Geociencias y Medioambiente, Carrera 80 No 65-223, Bloque M2, Office 312 - Campus Robledo, 050036, Medellín, Colombia

* PhD, Full professor, Juan Carlos Loaiza-Usuga, jcloaiza@unal.edu.co, ORCID iD: https://orcid.org/0000-0002-3821-7518

Abstract

The study site La Chorquina ravine is located in the northern part of the Colombian in the western Andes region, where three alluvial fans with different altitudinal levels have been identified, being one of them the object of this study. These sedimentary deposits have been associated with the "El Guásimo" landslide, a downstream deposit that was considered responsible for the damming of the Cauca River. Paleoenvironmental reconstructions carried out during the last years question the existence of paleolakes, and support the hypothesis of a typical alluvial plain dynamic influenced by the Cauca River tributaries. In this research, two profiles were subjected to a complete pedostratigraphic field characterization (structure, horizons differentiation, colour, porosity, and stoniness); Selected soil samples were submitted to physicochemical and mineralogical analyses, of which 11 micromorphological analysis were performed, and carbonates, gypsum, iron and manganese oxides, cutans, nodules, concretions and other pedological features were identified. The research proved the predominance of alluvial soils under an alluvial sedimentary environment with a predominance of features associated to the dynamic alluvial system characterized by little mineral alteration and similar mineralogical composition. The presence of carbonates and gypsum evidences seasonality changes in the climatic conditions. By means of the study of alluvial soils it is possible to identify paleoclimatic seasonality through edaphological records, which makes these soils a powerful tool for the study of Quaternary processes and paleoclimatic seasonality in tropical fluvial environments.

1. Introduction

Quaternary alluvial fans are characterized by the complexity of their genesis based on climatic and tectonic characteristics (Gómez-Villar, 1996; Kumar et al., 2007), being affected by slope conditions and lithology, with a radial distribution of the clasts in a decreasing sense as they move away from the apex (Colombo, 2010). Changes in the base level in response to tectonics or weather conditions can lead the fan to incise (Harvey, 2002; Kumar et al., 2007). Tectonic activity is considered to be critical in the control of alluvial fan sedimentation in active orogenic belts (Kumar et al., 2007; Viseras et al., 2003). Depending on climatic conditions, there may be variations between wetland fans and arid zone fans (Colombo, 2010; Benito et al., 2004).

The study area has been subject to various periods of anthropogenic occupation since 940 BP (Castillo, 1988). Humans altered forests from the Pleistocene / Holocene transition through plant dispersal and their concentration in anthropogenic patches, domesticating the forest (Aceituno and Loaiza, 2015), which favored the increase of sediment load (Vélez et al., 2013). Despite the biological and socio-economic importance of the Cauca river through history, aquatic ecosystems, hydrological behavior, sedimentological and climatically implications imposed by this fluvial system, are still poorly understood (Martínez et al., 2013; Valencia et al., 2017; Ceron et al., 2021). According to Vélez et al. (2013), the Cauca River's fertile floodplains, with their rich soils and highly productive lakes and swamps, are a vital resource for the economic and social development of the country. Several authors affirm that Cauca River in this sector was blocked by the Guásimo mega-slides (6.5°N, 75.5°W, 550 m.s.n.m.) that impounded the Cauca River, originating sedimentation processes modeling the terrace system (Page and Mattsson, 1981; Martinez-Sacristan, 2017). Ortiz and Pérez (1998) make a geological and geomorphological characterization of the Guásimo Megaslide. Page and Mattsson (1981) calculated the filling times of the three lakes through the varve method, used in cool temperate seasonal climates (Bradley, 1999); Mesa (2003) questions the use of this methodology in tropical climate zones with a bimodal regime and ENSO. The accumulation of sediments in the Cauca paleolake start 6000 BP; however, four deposition environments

were identified swamp, alluvial lacustrine, lacustrine and alluvial (García et al., 2011). For Velez et al. (2013) the evolution and dynamics of the ancient floodplain of the Cauca River and its aquatic ecosystems, were related to swamps and ponds on the floodplain formed for river connectivity; the establishment of lakes and swamps that were probably fed by seasonal flows of low energy. Several stratigraphic, geochemical, and organic matter studies of the late Holocene in relation to succession of the Cauca paleolake in the middle part of Cauca Valley, northern Colombia, suggests that it was deposited in a ria lake environment. (García-Castro, 2011; Martínez et al., 2013; Vélez et al. 2013; Martínez et al., 2015). These studies affirm that it was a laminated deposition correlated with ENSO variability (2000 to 1500 yr BP), which led to increased precipitation and to the transition from an igapo (black water) to a varzea (white water) environment. The La Chorquina Megafan offers a unique, high resolution record to understand the genesis and pedogenetic development of Holocene soils in a fluvial environment. Depositional dynamics correspond either to a single event (Cauca river damming) to several alluvial events. The micromorphological features will be correlated with sedimentary and/or edaphic processes, these allow the interpretation of the different formation environments, allowing the paleoenvironmental reconstruction of developed alluvial soils. In this study, we used several pedostratigraphical analysis and techniques to answer the scientific question: do the Quaternary paleosols of the La Chorquina creek reflect flood events of great magnitude associated with damming of the Cauca River or are they only the result of environmental changes or the hydraulic dynamics of the fluvial system? The general objective is to define the formation conditions and environmental changes of the terraces of La Chorquina from soil micromorphology. This study was focuses in the soils present in the two levels of the La Chorquina stream and their relationship with neighboring streams and study the genesis and evolution of the soils of La Chorquina fan in relation to changes in climatological conditions seasonality.

2. Materials and methods

2.1. Study area

The study area is located in the Chorquina creek (7.6 km channel), municipality of Santa Fe de Antioquia, eastern margin of the western Cordillera of the Andes, (Fig. 1). The study site is located between 1470 to 450 m a.s.l in the middle part of the Cauca river valley (south-north direction) with meandering alignment, and braided as a consequence of the pull apart basin configuration product of the combination of efforts of the fault systems (García et al., 2011; Vélez et al., 2013). The origin of the deposits corresponds to successive events of deposition of alluvial fans in a mountainous front; the occurrence of these geoforms under current geomorphological conditions would be limited by the short distance (2.67 km) from the mountain front to the deposit. These conditions necessarily imply a change in the base flow (Cauca river) due to tectonics or damming under more humid climatic conditions (high rainfall regime) than the current ones. The arrangement of the fans would break the basic principle of fluvial geomorphology "highest is the oldest"; according to Viseras (2003), in three superimposed levels of alluvial fans the oldest is found at the base (greater extension and a greater degree of dissection), and youngest fan is on the top of the sequence. In this case the height is related to the dominant tectonic regime during the deposition of the materials. Similar behaviors have been reported by Shukla et al. (2001) for the Ganha megafan. The climate is widely influenced by the Intertropical Convergence Zone (ITCZ), the trade wind pattern where rainfall varies depending on the location of the mountain ranges and circulation of humid winds comes from the East or the Southeast (Poveda et al., 2006). The rain has a bimodal regime (droughts December-March and July-August), with an altitudinal rainfall gradient with of 850–950 mm/year (Vélez and Rhenals, 2008). The relief has a marked influence on the spatial variability of the precipitation towards the bottom of
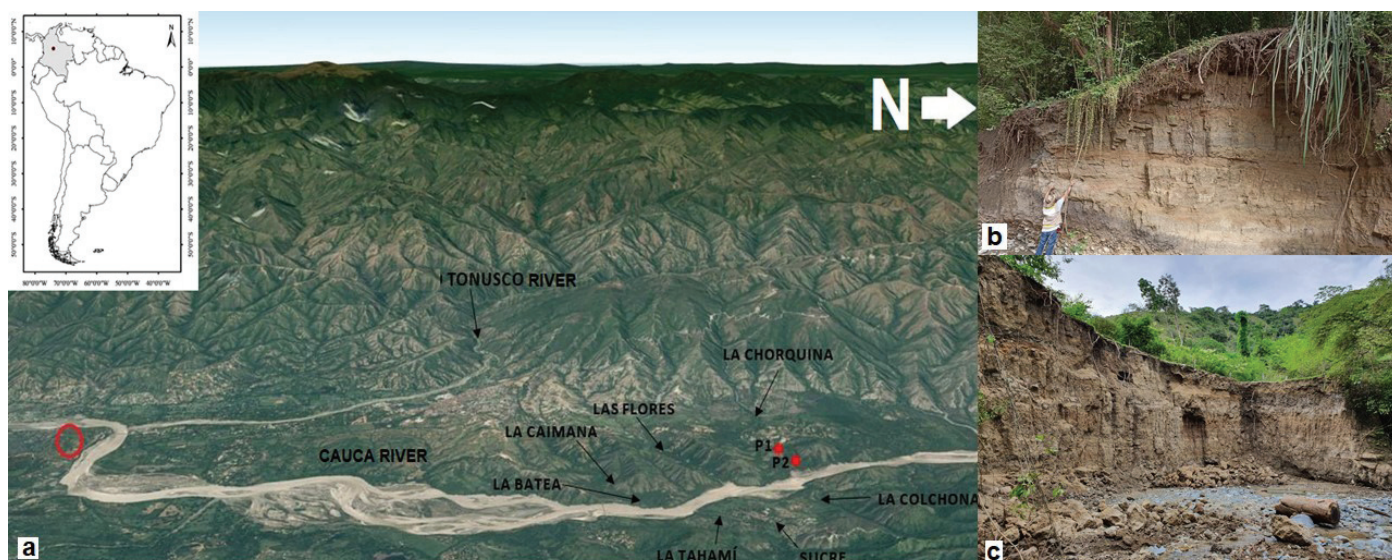

Fig 1. a) Location of the study area La Chorquina Catchment, b) Profile 1, c) Profile 2.

the Cauca river valley (475 m a.s.l) where the lowest values of precipitation are present (850–950 mm/year), this increases according to the elevation (2000 m a.s.l) reaching maximum values (2200 mm/year) in the highest areas (Espinal, 1992; Vélez and Rhenals, 2008). La Chorquina is located in the Tropical Dry Forest with a predominance of grasses and some relicts of gallery forest and xerophytic vegetation (Espinal, 1992).

2.2. Cauca river geological framework

In the area of La Chorquina, the Cauca river basin has a South-North direction, with a typically low sinuosity meandric alignment pattern and a short section braided towards the south; this change in the alignment pattern, according to Vélez et al. (2013), is a consequence of the pull-apart basin configuration in the area (Suter and Martínez, 2009; Suter et al., 2011), product of the combination of stresses associated with the Cauca Romeral fault system (c.f. Vinasco and Urbani, 2012), which comprises anastomosed faults with a predominant NNW direction, and represents the limit between the Western and Central Cordilleras. Tectonic activity in the area affects Quaternary deposits (Paris et al., 2000; Suter et al., 2011). In this part of the Cauca river basin, the Cretaceous oceanic Barroso Formation and the Santa Fe Batholith, and the Oligocene-Miocene Amagá Formation are the main geological units (González, 2001). The less well defined more recent units are the El Tunal, Goyas, Anzá and El Llano sedimentary sequences.

The Barroso Formation is composed of basic volcanic rocks of Cretaceous age that outcrop on the eastern flank of the Western Cordillera; the basic volcanic component formed by intense oceanic volcanism in an ophiolitic sequence, with aphanitic, porphyritic rocks, basaltic and andesitic spills, diabase, spilite, pillow lavas, with pyroclastic rocks such as agglomerates, breccias, and tuffs, interbedded with concordant lenses of siltstones, claystone, and black chert (Rodríguez and Arango, 2013).

The Santa Fe Batholith is a tonalitic unit that intruded Triassic rocks from the Central and Western Cordilleras of the Colombian Andes (Nivia and Gómez-Tapias, 2005); this intrusive body has an assigned age between 100 and 90 Ma, product of partial melting of mafic mantle rocks of the Colombian-Caribbean Ocean Plateau (CCOP) (Weber et al., 2015). This unit is composed of tonalites, quartz-diorites, gabbro's and diorites. Tonalite the most abundant rock, intruded by late dioritic dikes (Weber et al., 2015).

The Amagá Formation is fluvial siliciclastic sedimentary formation that has been divided into two members (see Silva-Tamayo et al., 2020 and references therein): the Lower Member, with conglomeratic banks, sandstones, conglomeratic sandstones, slaty claystones and sporadic coalbeds; the Upper Member comprises coarse-grained sandstones and siltstones, without coalbeds. The rocks of the Amagá Formation have a high degree of consolidation and well sorted materials, with well-defined bedding planes.

Locally the Amagá Formation is overlain by se series of sedimentary sequences. These are: 1) El Tunal Sequence, that consists of an alternation of coarse to very coarse conglomerates in a sandy matrix and intercalations of coarse sandstone strata with gravel, locally with calcareous cement. The composition of the clasts corresponds to 98% dioritoids and 2% basalts. The composition of the matrix corresponds to rock fragments and minerals such as calcic- plagioclase, epidote and hornblende (Parra-Sánchez, 1997). 2) The Goyás Sequence, composed of silty sandstones, clayey siltstones, occasional peat lenses, and conglomerates with clasts less than 10 cm (Parra-Sánchez, 1997). 3) The Anzá Sequence, made up of clast-supported conglomerates composed of more than 60% of green aphanitic basalts and white quartz, occasionally with andesites and tuffs from the volcano-sedimentary Combia Formation. These conglomerates are alternated with conglomeratic sandstones and silty sandstones (Parra-Sánchez, 1997). 4) El Llano sequence, composed for different strata, with phyllosilicates, amphiboles, opaque, quartz, feldspars, lamprophyre, glass, limonite, volcanic ash, tuffs, tuffite and rock fragments, clayey silt texture; the silts have abundant phyllosilicates and plant remains (Parra-Sánchez, 1997).

2.3. Field description and sampling

Sampling sites were selected based on studies conducted by Mesa (2003), Suter et al. (2011), García et al. (2011), Vélez et al. (2013) and Johnstone (2014), two representative profiles located in the lower part of the La Chorquina stream were selected. The alluvial deposits where described in the field; and complete stratigraphic characterization was doing through different levels of the alluvial fan deposit. The description of the soil profiles was carried out according to the criteria of soil survey manual (SSS, 2018), the classification according to the Key to soil taxonomy (SSS, 2014) and IUSS Working Group WRB (2022). The detailed description of the sedimentary materials also included the identification of sedimentary facies indicating dissimilar paleoenvironments in terms of humidity and pedogenesis and the lateral variations of the facies, in order to mark and correlate the events that could represent abrupt changes in the system or contributions of materials to them (Olivera et al., 2004). Each soil profile was sampled for chemical, physical and mineralogical analyses, as well as for micromorphology according to Loaiza-Usuga and Poch (2015) and Soil survey manual (SSS, 2018) methodologies.

2.4. Laboratory analyses

A total of 36 soil samples were taken, 10 in Profile 1 and 26 in Profile 2. Soil samples were analyzed in the soil laboratory of Universidad Nacional de Colombia – Medellín (Colombia). Size distribution of mineral particles (≤2 mm) was analyzed by Bouyoucos method (Day, 1965), soil reaction was measured with a potentiometer (827 pH Lab Metrohm®) on a 1:1 soil-water ratio, organic carbon was analyzed by moist digestion (Walkley and Black, 1934). According SSS (2004) cation-exchange capacity (CEC) and extractable bases were measured on a sample percolated with ammonium acetate 1 N at pH 7.0. Available phosphorus was measured with modified Bray-II method (Bray and Kurtz, 1945). For mineralogical analysis of the sand fraction, the dry sieving procedure was carried out by means of mechanical separation of the sand contents, and the fine fraction by means

3

of a 200 mesh (0.074 mm), according to the Porta-Casanellas procedures (1986). Soil samples for sand fraction mineralogical analysis were studied with a petrographic microscope (Axio Lab-A1 Zeiss®) according to Tauler and Canals (2015) counting 300 grains per sample. The undisturbed soils samples for micromorphology were dried for six weeks at room temperature, and impregnated with polyester resin and let harden for another six weeks. Slabs were cut with a diamond disc and polished with a polishing machine (Thin Sectioning System Petrothin Buehler Ltd®) to obtain a thickness up to 20 μm. Thin section description and interpretation were carried out with an Axio Lab-A1 Zeiss® microscope, and were based on Stoops (2021) and Loaiza-Usuga et al. (2015).

3.   Results

3.1.   Alluvial deposits

In the study site the lower fan corresponds to a yellowish-brown and gray deposit (product of changes in the water regime of the sequence) where fine sand-sized particles predominate and a smaller proportion of silt with very few blocks (≤ 10 cm), fine parallel lamination, and bands of thin irregular iron layers. The matrix/block ratio in this deposit corresponds to a mud flow with non-Newtonian behavior (Bingham plastic fluid); its granulometry and composition is similar to the material of the active channel (La Chorquina creek). However, the active stream deposit has little matrix and a larger number of blocks. This fan was deposited under wetter conditions than today. The boundary between middle and low fan is an erosional surface.

The middle fan corresponds to yellowish-brown silty sand deposit, without lamination, with an easterly inclination of 6° and thickness ≥ 35 m. This fan has lower matrix content than the lower fan; diorite blocks was smaller (≤ 4 cm diameter) and angular than in the upper fan. The dissection degree is medium; and there are undulations on the surface that give rise to a very smooth hilly relief. The predominance of the matrix over the block content indicates a behavior of non-Newtonian flow dynamics (Bingham fluid). In surface this fan is overlain by the most recent and less extensive upper fan. Washing and accumulation of poorly cemented calcium carbonates and sulfates is common.

The upper fan rests on the conglomeratic silty sandstones and the Goyás conglomerate sequence (Upper Miocene – Pliocene), they are gray and reddish materials, and these colors show different dominant edaphic processes. This fan has east inclination of 3°–6°, with a medium degree of dissection and undulations that form a very smooth hilly relief, it reaches 35 m in thickness. Alluvial fans are the typical landform in the Cauca mountain front, characterized by blocks in a fine matrix associated to torrential flow; some fan relics (affected by alluvial erosion) are observed on the right bank of the Cauca River.

3.2.   Pedostratigraphic characterization

The soils are derived from mixed alluvial and colluvio-alluvial deposits, they are moderately deep to shallow with abrupt and plane limits and limited by stoniness. Soils are well drained with medium to moderately fine textures. Towards the base of the profile, fine granular materials predominate with a parallel and horizontal lamination with an inclination of 3–6° (Fig. 2a), towards the upper part there is a clear fluvial influence, with
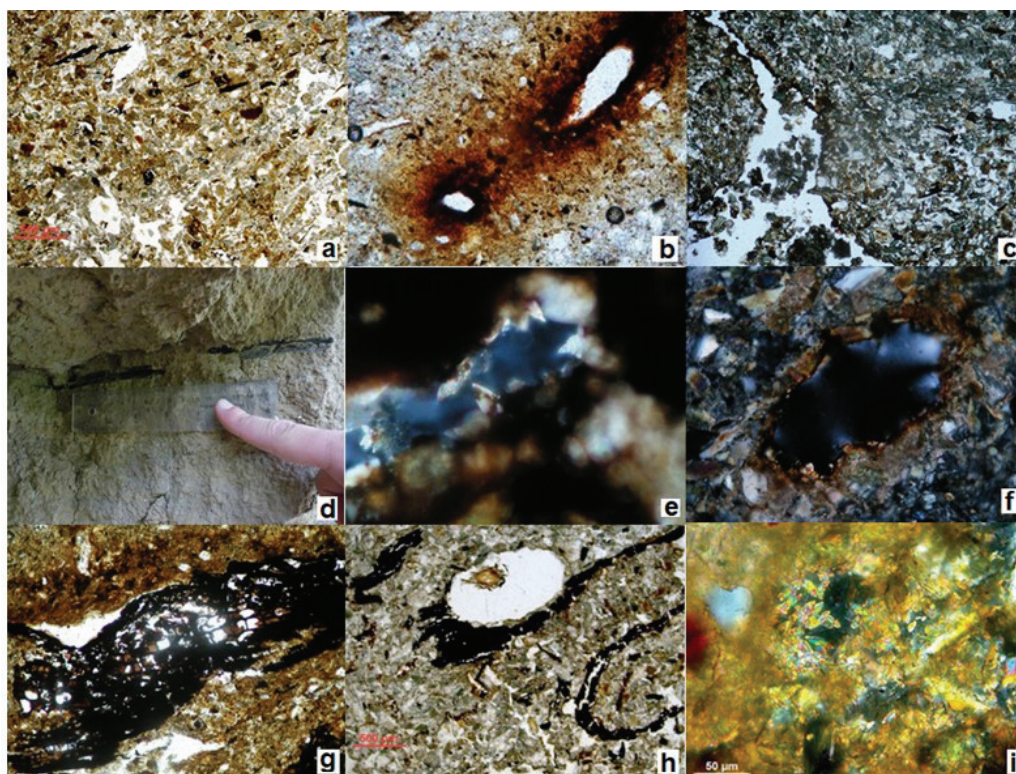
Fig 2. a) Minerals with very little alteration from the upper part of the basin with microcharcoal from local fires; horizontal lamination with inclination (PPL), b) Iron internal hypocoatings associated to hydromorphic conditions 4x (PPL), c) Charcoal fragments of direct burning remains 20x (PPL), d) Macro charcoal in alluvial deposit, e) Pseudomorphs of calcite, replacement of lenticular gypsum crystals by calcite (high order interference colors and the crystallographic symmetry) 4x (XPL), f) Juxtaposed hypocoatings of calcite and iron oxides 20x (XPL), g) Plant tissues 10x (PPL), h) Root channels with tissues, soil aggregates and charcoal fragments 4x (PPL), i) Gypsum crystals (50 μm)

sands and a cross stratification. The other horizons correspond to changes in the hydrological regime that favors the remobilization of iron oxyhydroxides under oxidation reduction conditions, giving rise to stagnic and gley horizons (under reduction conditions). Table 1, shows the most relevant characteristics described during the detailed survey of the pedostratigraphic column, color, soil structure, pedofeatures, limit and HCl reaction. In profile 1 the materials are silt-clayey with the presence of sand at the top of the B_1. The presence of pedotubules in B_4 are related to high organisms' activity. The phenomena associated with redoximorphic conditions (Fig. 2b) are more evident in Bg_1 and Bg_2, where carbonation is observed. The presence of charcoal (finer material) is common in various horizons (Fig. 2c, 2d), being more abundant in Bg_1, where it is laminated with defined orientation, reaching a thickness of up to 1 cm. The structure of all horizons is coarse angular to subangular blocky without structure in the less weathered materials. The B_2, B_3, Bg_1 and Bwk horizons have the presence of calcite associated with root channels; and presence of gypsum crystals in B_2 (Fig. 2e, 2f). B horizons have pedofeatures than bioturbation structures, remobilization of calcium carbonates inside the profile (high reaction to hydrochloric acid), mottled by oxidation reduction processes (olive and grayish gley matrix) with sporadic presence of fine sand-sized charcoal and laminated materials rich in fine and very fine sand, laminations of organic matter (OM) associ-

ated to alluvial deposition. This soil profile is characterized by fine textures, with a neutral to moderately alkaline pH, with low electrical conductivity (EC) throughout the soil profile, except for B_2 (high EC), the OM content is low, and the calcium and magnesium contents are very high. The potassium is low to very low, sodium fluctuates from medium to high, and phosphorus is low to medium. The B_2 horizon tends to be a salt-affected soil.

The Profile 2 has crumbly structures on the surface, subangular blocks, columnar for materials with greater pedogenesis, loose grain, laminar tendency and no structure for the less pedogenetically altered materials. This profile has a greater granulometric variation with a clear fluvial influence in the upper and middle part of the stratigraphic sequence. This soil has contrasting coarse, fine, and medium textures up to 11.2 meters deep, from there, silty and loamy clay textures predominate (11.2 to 13.5 m). At C_1, Bg_1, and C_2 horizons there are a parallel lamination; with cross-stratification at Cg_{12}, C_3, Ab_7g_{13}, and Cg_{14} horizons. These gravel and sand lenses of alluvial origin, as well as lenses with parallel lamination and cross-stratification of sands and clays, enriched with organic matter, with horizontal accumulation of iron oxides (incipient irregular iron thin layer horizon). The Cg_{12} horizon has subrounded gravels ($\leq$ 6.5 cm diameter) with redox evidences and imbrication to the East. The gley and stagnic matrices with olive, gray and brownish colors, and strong reaction to hydrochloric acid (due to carbonation processes).

Table 1
Morphology of soil profiles 1 and 2, La Chorquina alluvial fan

Profile 1						
Hz	Depth	Munsell color	Structure	pedofeatures	Limit	HCL reaction
	(cm)	(moist)				
Ap	0–30	10YR3/2	T, Sbl, Ld	Frequent root channels and fine roots; Lithics fragments ≤ 3cm	C, S	Non-calcareous
Bw_1	30–200	5Y5/2 (70%) 10YR6/8 (20%) 5Y7/2 (10%)	Sbl	Fine parallel lamination	A, S	Non-calcareous
Bw_2	200–216	10YR6/6 (60%), 5GY6/2 (40%)	C, Abl, S, Cm	Green fine parallel lamination	C, S	Moderately calcareous
Bw_3	216–229	2.5Y4/2	C, Abl, S, Cm	Fe oxides lamination, fresh OM, high selection	A, S	Moderately calcareous
Bw_4	229–238	2.5Y7/4 (60%) 2.5Y6/1 (40%)	C, Abl, S, Cm	Laminations of organic matter and $CaCO_3$, Muscovite and $CaCO_3$ only present in laminations. High selection, frequent pedotubules	C, S	Moderately calcareous
Bw_5	238–242	2.5Y4/1 (70%) 2.5Y6/1 (30%)	C, Abl, S, Cm	Green parallel lamination	C, S	Moderately calcareous
Bw_6	242–250	Gley1 5/5GY	C, Abl, S, Cm	Fine parallel lamination, remobilization of $CaCO_3$ inside root channels (≥ 2mm diameter)	A, S	Moderately calcareous
Bw_7	250–252	5Y2.5/1	C, Sbl	Transitional layer rich in OM, layers with gray clay in the upper part and concentrated in the base; mottled root channels, highly bioturbated	C, S	Slightly calcareous
Bw_8	252–258	Gley1 4/5GY	C, Sbl	Fe Oxides mottled, highly bioturbation, profile high content of muscovite	C, S	Non-calcareous
Ab_2	258–297	Gley1 4/N	C, Sbl	Fine charcoal random distributed	C, S	Non-calcareous
C_2	297–X	7.5YR5/3	-	-	C, S	Non-calcareous

Table 1 – cont.

Profile 2						
Hz	Depth	Munsell color	Structure	pedofeatures	Limit	HCL reaction
	(cm)	(moist)				
Ap	0–45	10YR3/2	Crb, F, Ld	Frequent root channels and fine roots, Fe oxides in root channels, lithic fragments (≤ 3 cm diameter)	C, S	Non-calcareous
Bw	45–70	2.5Y5/3	Sbl, M, Ld and T, Cls, C, Ld	Few fine root channels and vertical fresh and decomposed roots, frequent charcoal fragments, lithic fragments (≤ 3 cm diameter)	A, S	Non-calcareous
C_1	70–230	Gley1 4/5G/1	Ns	Frequent fragments of diorite, tonalite and mylonite, crystalline and white quartz, bioturbation evidences, frequent lithic fragments, nodules Mn oxides, coarse sands	A, S	Non-calcareous
Bg_1	230–280	2.5Y6/6(70%) Gley1 4/5G/1(30%)	Sbl, Ld	Incipient lamination (>5mm), frequent very fine channels and root channels with Fe oxides coatings and infillings, few horizontal and vertical roots channels, small lenses with sand fillings, low selection	C, S	Moderately calcareous
C_2	280–294	5Y6/4(60%) Gley1 5/5GY (40%)	Ns	Parallel fine lamination, deposition planes, few root channels, frequent root channels with Fe oxides coatings	A, S	Non-calcareous
Bg_2	294–346	5Y6/4 (60%) Gley1 5/5G (40%)	T, Sbl, Ld	Parallel lamination, frequent root channels with Fe oxides coatings and infillings, frequent cracks	C, S	Moderately calcareous
Cg_1	346–368	2.5Y5/4 (60%) Gley1 4/5G (40%)	Ns	Oxide reduction laminated sands, few root channels and frequent fine roots, frequent root channels with Fe oxides coatings, leaf footprint (*Gramineae*), good selection	A, S	Moderately calcareous
Abg_1	368–430	2.5Y6/4 (70%) Gley 5/10GY (30%)	Co, T, C, M, Sbl, Ld	Few to frequent root channels and frequent root channels with Fe oxides coatings and infillings (2.5YR4/8, 2.5YR3/6), horizontal charcoal (5 mm diameter), Fe nodules and fragments (5YR5/6), low selection	C, S	Non-calcareous
ABg_1	430–560	Gley1 6/5GY (95%) 7.5YR5/6 (5%)	T, Cls, M	Few to frequent root channels, few fine roots, rest of roots (2.5YR3/6), abundant fine root channels with Fe oxides coatings and infillings frequent fine charcoal oriented horizontally, redoximorphic features, low selection	C, S	Extremely calcareous
Cg_2	560–587	2.5Y6/4 (80%) Gley1 4/5GY (20%)	Ns	Few root channels and fine charcoal, abundant fine root channels with Fe oxides coatings and infillings, calcite crystals, low selection	C, S	Moderately calcareous
Abg_2	587–639	Gley1 5/10GY	T, Sbl	fine root channels with Fe oxides and calcite infillings, abundant fine roots, radial gypsum aggregates, root channels with $CaCO_3$ infillings, frequent charcoal (≤ 5mm diameter)	C, S	Extremely calcareous
Abg_3	639–670	Gley1 5/10Y	T, Sbl	Abundant root channels with Fe oxides coatings and infillings, radial gypsum aggregates, abundant fine and frequent coarse charcoal (≤ 3cm), low selection	A, S	Non- calcareous
Abg_4	670–710	2.5Y7/3 (50%) Gley1 6/10Y (50%)	Sbl, C, T, Cls	Root channels with OM infillings, abundant to frequent root channels and chambers with Fe oxides coatings, few mottles, few gypsum crystals, few fine roots, pedogenetic wetting and drying cracks, placic horizon, low selection	A, S	Non- calcareous
Abg_5	710–760	Gley1 5/10Y	Sbl, C, T, Cls	Coarse and medium root channels with Fe and Mn oxides coatings and infillings, abundant nodules Fe and Mn oxides (1mm), frequent fine and very fine root channels, chambers with OM coatings, pedotubules dense infilling, placic horizon	A, S	Non-calcareous

Table 1 – cont.

Hz	Depth	Munsell color	Structure	pedofeatures	Limit	HCL reaction
	(cm)	(moist)				
Abg$_6$	760–845	Gley1 6/N	T, Sbl	Parallel fine lamination, abundant root channels, abundant Fe oxides coatings and infilling in root channel, frequent Fe and Mn oxides infilling in fine root channels, frequent leaf footprint (*Gramineae*) oriented horizontally, low gypsum crystals, sub-rounded igneous lithics blocks in the base ≤ 6.5 cm diameter	A, S	Non-calcareous
Cg$_3$	845–857	Gley1 5/10Y	Ns	Subrounded gravels ≤ 3 mm diameter inside silty matrix	A, S	Non-calcareous
C$_3$	857–909	2.5Y4/3 (60%) 2.5Y5/2 (30%) Gley2 4/10BG (10%)	Ns	Frequent Mn oxides, few fine roots, few fine char-coal, sandy clay horizontal lenses with gypsum crystals, frequent gypsum crystals, cross stratifica-tion, low selection	A, S	Non-calcareous
Abg$_7$	909–939	Gley1 4/10Y (30%) Gley1 4/5GY (30%) 2.5Y5/4 (40%)	Sbl, M	Root channels with Fe and Mn oxides, lenses and root channels with Fe oxides coating and infilling, Clays with fine parallel lamination and good select-ed sand lenses, lenses rich in OM in upper part of the horizon, strong gleization	A, S	Non-calcareous
Cg$_4$	939–1119	Gley1 4/10Y	Sbl, C, Ld	Root channels with Fe and Mn oxides, Parallel lami-nation, bioturbation, frequent gypsum crystals and Mn oxides (Pyrolusite), irregular layer and sand stratification, gypsum radial aggregates inside pe-dotubules, low selection	A, S	Non-calcareous
Abg$_8$	1119–1175	Gley1 5/N (60%) 5Y6/2 (40%)	T, Sbl, M	Root channels with Fe oxides, abundant roots slight-ly decomposed, frequent leaf footprint (*Gramineae*) oriented horizontally, pedotubules infilling with soil mineral material, sand concretions	A, S	Non-calcareous
C$_4$	1175–1245	2.5Y6/4	Ns,	Parallel inclined laminated fine sands and lens of coarse gravels, accumulation of charcoal upper part, placic and Fe oxides fragments (horizontal) in the base	C, S	Non-calcareous
Abg$_9$	1245–1299	Gley1 5/10Y (50%) Gley1 5/N (25%) 5YR5/1 (25%)	Sbl, M, T, Cls	frequent Fe oxides coatings in root channels, verti-cal roots, lens of Mn oxides (globular pyrolusite), charcoal, Fe oxides, abundant Mn oxides associ-ated to gypsum and sulfur, placic horizons, burn layer in the upper part of the horizon rich in char-coal	A, S	Non-calcareous
Cg$_5$	1299 -1315	2.5Y5/4 (90%) Gley 5/10GY (10%)	T, Sbl	Few root channels wit Fe oxides, frequent Mn ox-ides, parallel fine lamination and sandy lens, good selection	A, S	Non-calcareous
Abg$_{10}$	1315–1335	Gley 6/N (90%) Gley 2.5Y6/3 (10%)	T, Sbl, F	Vertical root channels with Fe oxides and sand in-fillings, preserved organic rests cover by Fe oxides, stagnic matrix, hard horizon	C, S	Non-calcareous
Cg$_6$	1335–1349	2.5Y6/4 (80%) 2.5Y6/3 (20%)	T, Abl, C	Abundant Fe oxides, parallel fine lamination	C, S	Non-calcareous
C$_5$	1349–X	2.5Y6/4	Ns	Frequent roots channels with Fe and Mn coatings, frequent fragments of placic (1mm), frequents to few roots' channels, frequent fine roots, parallel fine lamination, massive, good selection	-	Non-calcareous

Ns: not structure, Abl: angular blocks, Sbl: subangular blocks, Crb: Crumby, Cls: Columnar, Pl: platy, Ld: low developed, F: fine, C: coarse, M: medium, Co: compacted, S: slightly, T: tendency, OM: organic matter, A: abrupt, C: clear, S: smoot.

The C3 is composed of sand and gravel. The profile 2 show intercalations of finer materials (silty clay) with evidence of redoximorphic conditions with two phases: phase I corresponding to the Ab_2g_7, Ab_3g_8, Ab_4g_9, Ab_5g_{10} and Ab_6g_{11} horizons, phase II is composed of the Ab_8g_{15}, C_4, Ab_9g_{16}, Cg_{17}, $Ab_{10}g_{18}$, Cg_2 and C_5 horizons. In these finer materials Ab_6g_{11}, C_4, Cg_{17}, Cg_{19} and C_5 horizons have a thin parallel lamination. The presence of grass molds in the Cg_3, Ab_6g_{11}, and Ab_8g_{15} horizons is common, as well as remains of vertical trunks in $Ab_{10}g_{18}$, which indicates periods of stability (pauses in deposition) long enough for the development of vegetation and incipient pedogenetic processes. The well-preserved roots and plant tissues were covered with iron oxides, pedotubules filled with material from the same horizon, sands and iron oxides; with root channels filled with iron and manganese oxides and charcoal fragments. In the lower and middle levels root channels filled with iron oxides, fine sands and calcite are common; including the presence of individual and radial aggregates of gypsum crystals in the Ab_2g_7, Ab_3g_8, Ab_4g_9, Ab_5g_{10}, C_3, Cg_{14} and Cg_6 horizons (Fig. 2e, 2f). The presence of gypsum crystals sometimes is accompanied by the presence of accumulations of sulphurous materials, recarbonation processes, iron and manganese oxides, the latter can be abundant in some horizons in the form of globular pyralusite. The remains of charcoal in Profile 2 reach several centimeters as in the C_2 (7 cm), Ab_6g_{11} (6 cm) and Ab_9g_{16} (9 cm) horizons; charcoal was depositing horizontally following the lamination of the horizons. The pH is neutral to moderately alkaline in the first 7 m depth. From a depth of 7 m they tend to be moderately to slightly acidic at depth. Electrical conductivity tends to be very low at the top of the profile, medium in the middle part of the profile increasing at high EC values towards the bottom. The values for organic matter are high for most of the horizons, except for Ab_8g_{15}, which presents medium values. Calcium and magnesium contents are very high while potassium is very low to low, sodium fluctuates from medium to high and phosphorus is medium in the profile with high contents in Abg_5. Sodium increases its values in depth, the CICE is high throughout the profile. A detailed physicochemical characterization of the study soil profile is showed in the Table 2.

3.3. Mineralogical proxy

The sedimentary deposit is composed of silty and sandy materials with parallel inclined lamination at the base, grading to silty sand and cross-laminated sand in the middle part (profile) to silt with gravel and blocks in the upper part of the profile, which shown its alluvial origin. Sand mineralogy had the presence of lithic fragments of diorite and fine-grained sedimentary rocks, with minerals such as hornblende, epidote/zoite/clinozoite, feldspars, quartz, muscovite, biotite with little alteration (little weathered), Table 3. The main source of materials is the upper part of the basin (mountain range). For profile 1, the first three horizons (Ap, B_1 and B_2) have a very marked presence of lithic diorite fragments (maximum 72.82%); only in the B_2 there is 11.65% of lithic fragments of sedimentary rock. From the B_3, the presence of charcoal is evident in the B_2 horizon reaching 22.7% as maximum.

Profile 2 had a highest content of diorite fragments in the upper part of the sedimentary sequence; in the C_2 horizon the maximum value (diorite) is 30.6% with lesser values for C_1 (18.1%), Cg_6 (6.8%) and Cg_{14} (7.7%). The lithic fragments of sedimentary rocks were found in the lowest part of the sequence in Cg_{14} (13.31% maximum value). The alluvial materials were the source area of the sediments of both deposits (profile 1 and 2), the source were Santa Fe Batholith rocks and reworked Tertiary fans materials (with the same parent material) from the middle part of the basin. To summarize, hornblende was ≤ 1%, the dominant mineral is sericite (40%), and in smaller proportions orthoclase, quartz, and biotite with medium to high degree of alteration.

3.4. Micromorphological features

The most important micromorfological features of the samples analyzed are discussed in this section; the micromorphological features are illustrated in the Fig. 2. In the study profiles the soil has alternation of single grain microstructure (monic) interspersed with combination of coarse and fine components inside laminations (open to double spaced porphyric). There is weakly to strongly developed subangular blocky primary microstructure, partially accommodated; single grain to platy secondary microstructure. Simple and complex packing voids, root channels, chambers, vesicles and planes were found. The micromass was grey, brown yellowish and reddish brown. There is presence of hypocoatings and coatings (Fig. 2b, 2f), loose discontinuous infillings, typic coatings, layering and compound layering of calcium carbonates, gypsum, iron and manganese oxides inside channels (Fig. 2e, 2f). Soil impoverishment pedofeatures are associated with translocation and accumulation of iron oxides. Low weathered in minerals, even in the feldspars, mineralogy of the coarse fraction was very homogeneous. The most important organic components were charcoal, oriented, tissues, calcium oxalate phytoliths, earthworm excrement, diatom remains, opaline phytoliths, last two only in Ab_3g_8 (Fig. 2a, 2c). Presence of wormholes, roots and cavities of soil invertebrates was common. Some plant tissues are well preserved and the groundmass shown evidence of gleization (Fig. 2g).

Profile 1 has subangular blocky and a single grain microstructure, double-spaced closed porphyritic, porostriated. There is presence of root channels rough and partially arranged root channels and chambers. There are coatings and hypocoatings of micritic calcium carbonate and gypsum, and juxtaposed typic coatings of non-laminated clays (Fig. 2i, 2j). It was found partially accommodated root channels (≤ 700 μm), coatings and hypo-coatings of iron oxides, chambers associated with fauna passage dense complete sand infilling, and preserved plant remains; and evidences of mixing of the original soil by organisms. Parallel lamination (marked by the orientation of the hornblendes) of silt and fine charcoal with inclination of 6° between the B_5 and Bg_1 horizons are found.

The upper part of profile 2, there is a common presence of microstructures in very thick subangular blocks, weakly separated and partially arranged. It is loosely grained with an

Table 2
Physical chemical analysis profile 1 and 2, La Chorquina alluvial fan

Profile 1														
Hz	Depth	Sand	Silt	Clay	Textural	pH	EC	OM	Ca	Mg	K	Na	P	ECEC
	cm	%			Class	1:1	dS m^{-1}	%	Cmol/kg				Mg/kg	
Ap	0–30	28	36	36	clay loam	7.0	0.13	1.3	20.2	7.3	0.26	0.32	18	29
Bw$_1$	30–200	54	26	20	sandy clay loam	6.1	0.47	2.0	13.4	5.4	0.55	0.25	17	19.6
Bw$_2$	200–216	38	30	32	clay loam	7.8	4.87	0.80	36	19	0.14	5.45	25	60.6
Bw$_3$	216–229	32	42	26	Loam	7.7	1.09	0.66	28.5	10.3	0.13	1.07	26	40
Bw$_4$	229–238	30	42	28	clay loam	7.9	0.83	1.1	12.8	10.2	0.09	1.23	27	24.3
Bw$_5$	238–242	32	38	30	clay loam	8.0	0.36	0.99	18.3	7.6	0.11	0.95	29	27
Bw$_6$	242–250	36	36	28	clay loam	8.0	0.25	0.93	18.7	7.7	0.11	0.62	24	27.1
Bw$_7$	250–252	36	34	30	clay loam	8.1	0.22	1.2	19.6	8.2	0.12	0.60	28	28.5
Bw$_8$	252–258	14	52	34	silty clay loam	8.0	0.26	1.1	19.9	8.1	0.12	0.82	33	28.9
Ab$_2$	258–297	22	48	30	clay loam	8.1	0.26	1.0	21.1	8.5	0.11	0.65	30	30.4
C$_2$	297–X	26	40	34	clay loam	8.2	0.16	1.1	21.6	7.2	0.06	0.44	26	29.3
Profile 2														
Ap	0–45	28	36	36	clay loam	7.0	0.13	1.30	20.8	7.6	0.28	0.32	18	29
Bw	45–70	54	20	26	sandy clay loam	7.5	0.16	0.67	17.6	7.9	0.20	0.32	24	26
C$_1$	70–230	80	12	8	loamy sandy	8.5	0.12	0.21	10.7	2.0	0.10	0.23	16	13
Bg$_1$	230–280	54	26	20	sandy clay loam	8.0	0.08	0.28	17.7	5.5	0.11	0.31	21	23.6
C$_2$	280–294	76	10	14	sandy loam	8.1	0.18	0.14	14.3	4.8	0.10	0.30	23	19.5
Bg$_2$	294–346	34	38	28	sandy clay loam	8.4	0.18	0.52	26.6	8.4	0.16	0.50	17	37.7
Cg$_1$	346–368	54	24	22	sandy clay loam	8.5	0.16	0.19	18.8	6.8	0.14	0.55	25	26.3
Abg$_1$	368–430	28	38	34	clay loam	8.1	0.24	0.97	21.4	8.7	0.23	1.10	34	31.4
ABg$_1$	430–560	26	44	30	clay loam	7.6	3.40	0.61	38	8.3	0.19	1.87	20	48.4
Cg$_2$	560–587	66	16	18	sandy loam	7.7	0.91	0.20	15.7	5.3	0.12	0.53	38	21.7
Abg$_2$	587–639	10	50	40	silty clay	7.7	1.55	1.30	29.6	9.5	0.19	0.84	32	40.1
Abg$_3$	639–670	12	38	50	clay	6.8	1.36	1.20	27	11	0.22	0.76	33	39
Abg$_4$	670–710	14	40	46	silty clay	6.9	0.67	1.40	25.5	10.2	0.24	0.68	28	36.6
Abg$_5$	710–760	10	52	38	silty clay loam	7.1	1.82	0.59	24.5	9.4	0.18	0.65	42	34.7
Abg$_6$	760–845	8	50	42	silty clay	6.2	5.67	1.0	28.8	11	0.22	0.72	28	40.7
Cg$_3$	845–857	74	16	10	sandy loam	7.1	1.58	0.35	18.9	5.9	0.17	0.48	20	24.4
C$_3$	857–909	70	14	16	sandy loam	6.5	1.17	0.20	15.1	5.8	0.12	0.50	16	21.5
Abg$_7$	909–939	36	38	26	loam	5.9	2.10	1.10	16.9	7.1	0.19	0.57	25	24.8
Cg$_4$	939–1119	64	24	12	sandy loam	6.7	0.43	0.21	17	7.2	0.17	0.62	22	25
Abg$_8$	1119–1175	14	46	40	silty clay	5.9	4.43	1.70	30.1	10.7	0.26	0.87	32	41.9
C$_4$	1175–1245	40	34	26	loam	6.0	3.84	0.58	20.2	8.5	0.10	0.73	34	29.6
Abg$_9$	1245–1299	14	48	38	silty clay loam	5.7	3.70	1.10	23.2	10.2	0.19	0.92	38	34.5
Cg$_5$	1299 -1315	16	56	28	silty clay loam	6.4	1.58	0.47	21.4	8.8	0.17	0.82	36	31.2
Abg$_{10}$	1315–1335	16	44	40	clay loam	5.9	5.32	1.10	26.3	11.5	0.23	0.97	25	39
Cg$_6$	1335–1349	18	48	34	silty clay loam	6.3	5.33	0.48	24.2	10.6	0.19	0.86	36	35.9
C$_5$	1349–X	32	42	26	loam	5.9	3.82	0.56	22.2	5.6	0.18	0.87	30	28.9

Table 3
Mineral composition in the coarse silt fraction of the studied soils.

Hz	Depth (cm)	Lfg	Gm	Qz	Fp	M	FeO	CaCO$_3$	G	C
Profile 1										
Ap	0–30	+++	++	+	tr	–	–	–	–	–
Bw$_1$	30–200	–	+++	–	++	+	+	–	–	–
Bw$_2$	200–216	–	+++	+	++	–	tr	+	+	+
Bw$_3$	216–229	–	+	+++	+++	–	+	+	–	–
Bw$_4$	229–238	–	+	+++	++	+	+	+	–	–
Bw$_5$	238–242	–	–	–	–	–	–	–	–	+
Bw$_6$	242–250	–	++	+++	+++	–	–	+	–	+
Bw$_7$	250–252	–	–	–	++++	+++	–	+	–	–
Bw$_8$	252–258	–	–	–	++++	++++	+	–	–	+
Ab$_2$	258–297	–	–	++	+++	+++	–	–	–	+
C$_2$	297–X	++++	+	+++	++	–	–	–	–	–
Profile 2										
Ap	0–45	+	++	+++	–	+	+	–	–	–
Bw	45–70	+++	+++	++	++	+	+	–	–	+
C$_1$	70–230	++++	++	+	–	–	–	–	–	–
Bg$_1$	230–280	++	+++	++	+++	–	+	+	–	+
C$_2$	280–294	–	++++	++++	–	–	+	–	–	+
Bg$_2$	294–346	++	++	++	+++	++	+	+	–	++
Cg$_1$	346–368	+++	+++	+	+++	–	+	+	–	tr
Abg$_1$	368–430	–	–	+++	–	++	+	–	++	++
ABg$_1$	430–560	–	++++	–	+++	–	++	++	–	++
Cg$_2$	560–587	+	+++	++++	+++	–	+	+	–	+
Abg$_2$	587–639	–	+++	++++	–	–	++	+	++	+
Abg$_3$	639–670	–	+++	+++	++++	–	++	–	+	++
Abg$_4$	670–710	–	–	+	–	+++	++	–	+	++
Abg$_5$	710–760	–	–	+	–	–	++	–	+++	tr
Abg$_6$	760–845	–	–	+	–	tr	++	–	+	++
Cg$_3$	845–857	++++	–	–	–	–	–	–	–	tr
C$_3$	857–909	++	++	++	++++	–	–	–	++	+
Abg$_7$	909–939	++	++	+++	++	++	+	–	–	+
Cg$_4$	939–1119	–	++	+++	–	+++	+	–	++	++
Abg$_8$	1119–1175	–	–	–	–	–	+	–	–	++
C$_4$	1175–1245	+++	++	+++	–	–	+	–	–	++
Abg$_9$	1245–1299	–	–	++	+++	+++	+	–	++	++
Cg$_5$	1299 -1315	–	++++	+++	–	++	++	–	–	+
Abg$_{10}$	1315–1335	–	–	–	+++	–	+	–	+	++
Cg$_6$	1335–1349	–	–	+++	++	++	+	–	++	+
C$_5$	1349–X	–	+++	++++	–	+	+	–	+	tr

Lfg lithic fragments, Gm green minerals, Qz quartz, Fp feldspar, M muscovite, FeO iron oxides, CaCO$_3$ calcium carbonates, G Gypsum, C Charcoal, tr traces (< 1%), + present (5%–15%), ++ common (15%–30%), +++ abundant (30%–50%), ++++ more abundant (> 50%), – not found

inclined parallel lamination (6°–9°) marked by the orientation of the minerals and the charcoal, the lamination is a characteristic that is preserved throughout the entire profile. There are channels with dense complete infilling and cross microlamination of silt-clays and iron oxide coatings in brown, grayish brown, grey groundmass. Hornblende and fine charcoal, with low degree of alteration, are oriented. Root channels are inside a greenish groundmass with coatings and hypocoatings of Fe oxides (Fig. 2h). There is a gley horizon with vertical root canals in depth, horizontal planes, rubefacted calcium carbonate nodules, fan-shaped lamination produced by dehydration of mica, hornblende broken in steps, and abundant burnt organic structures. There are reddening and accumulation of globular manganese oxides. In depth was abundant preserved plant vascular tissues, moderately decomposed organic residues, coatings and hypo-coatings of Fe oxides. Redoximorphic pedofeatures, as well as, coatings, hypocoatings and infillings of iron oxides inside channels, calcium carbonates, gypsum, typical nodules of Fe and Mn oxides are observed in the overlying horizons. Gypsum infilling surrounding Fe and Mn oxides and iron oxyhydroxides are found. Biological activity is reflected by the presence of coprolites; some horizon presents remains of Bacillariophyceae diatoms, Naviculales order, Naviculales family, Pinnularia genus, characteristic of wet riparian zones and wetlands (Spaulding et al., 2010). There are coatings partially covered by lenticular gypsum crystals, typical Fe nodules, concentric, fingered, mamillated associated with plant structures; with typical and fingered Mn nodules and non-laminated clay coatings.

4. Discussion

4.1. Geomorphic environment

The mineralogical evidence shows that parent material, despite being deposited by alluvial phenomena, does not present any mineralogical trait related to the sediments of the Cauca River, which have a parallel lamination and a more varied composition. The origin of the sediments does not correspond to materials resulting from the damming of the Cauca River, but corresponds to the eastern flank of the Western Andes mountain range rocky materials, with predominance of rocks of the Santa Fe Batholith. The water level rise in the Cauca River product of the "El Guásimo" damming or the result of successive increases in the flow, would produce a counterflow that would favor the deposition of sediments from the Cauca River in the tributaries. The current river surface line analyzes of García (2011), García et al. (2011) and Serna et al. (2015) indicate a decrease in the relative water level of La Chorquina creek, in the middle and lower parts, as a result of the activity of the west Cauca and central Cauca faults. At the lower part of La Chorquina sedimentary sequences, there was an accumulation of Ca^{+2}, Mg^{+2}, Fe^{+2} cations as a result of the weathering of basic rocks, a dynamic favored by the low slopes and geomorphological conditions in this part of the basin; characterized by bottom valley conditions. The accumulation, composition and distribution of terrestrial carbonates

in semi-arid alluvial sedimentary environments are controlled by physical (transportation energy), morphological (slope gradient), chemical (precipitation, evaporation) processes and biochemical interactions (Nickel, 1985). The inclination of the fans towards the Cauca River, as well as the origin of the sediments evidenced by the stratigraphic columns and the geomorphology, show a sequence deposited from the mountain front and not a product of the damming of the Cauca River. Base level change, climate change, and changes in water and sediment load affect the developed time hierarchy of deposition discharge events (Shukla et al., 2001). The Cauca River has been an alluvial system that has had vertical variations throughout its geomorphological history. Other authors than Martínez et al. (2015) hypothesize; about the hydrologic change to higher-energy fluvial conditions could reflect periodic damming caused by the Cauca River, carrying a heavier sediment load, and thus forming the várzea-type lakes.

4.2. Soil genesis and classification

The first stage was characterized by the deposition of silt and clay particles (C_5 to Ab_8g_{15} horizons), showing a discontinuous sedimentation evidenced by exposure of plants tissues. For C_5, Cg_{19} and $Ab_{10}g_{18}$ horizons, pedogenesis starts under vegetation colonization conditions; subsequently Cg_{17} and Ab_9g_{16} were deposited followed by a period of stability and subsequently soil was developed. The increase in sediment load could have been the result of anthropogenic deforestation and a subsequent increase of precipitation events (Vélez et al. 2013). The presence of a horizon rich in coarse charcoal, evidences *in situ* burning of plant material, and a fast deposition which occurs in C_4 and Ab_8g_{15} horizons. Ab_8g_{15} has higher contents of organic matter, high content of Ca, Na, high electric conductivity, which make evident dry environmental conditions under moderate pedogenesis and base-poor parent material.

Subsequently, a cycle of deposition of sandy materials occurs, interrupted by the deposition of Ab_7g_{13} with lower ionic composition. The later C-horizons correspond to a phase of rapid and continuous deposition of materials; the following Ab horizons were related to cycles of deposition of silt-clay materials and greater pedogenetic stability evidenced by higher contents of OM, phosphorus, bases and higher pH values. The most important pedogenetic processes were a greater accumulation of organic matter, calcium carbonate precipitation (nodules, laminations and infillings), gypsum crystals and aggregates, reduction/oxidation processes and presence of pedotubules, root channels and edaphoturbation product of the organisms action. According to Buol et al. (2011), the solubilization of carbonates occurs during the rainy season; whereas dissolved bicarbonate migrates within the soil profile to some depth and reprecipitates during the following dry season. The wet season is responsible for the liberation of iron and lixiviation of bases by weathering (Duchaufour, 1982). The increase of pedogenesis in the floodplain was related to less frequent high-energy flows that formed ephemeral evaporitic swamps (Vélez et al., 2013). Water dynamics were associated to the presence of gley and stagnic matrix product of water accumulation processes in the soil pro-

file; these horizons are mottled, product of accumulation of iron and manganese oxides. The recarbonation processes are observed in root channels and iron oxide coating surfaces which evidence drier climate conditions. Alluvial fans frequently contain carbonate precipitates especially under semi-arid climates (Nickel, 1985). The presence of gypsum crystals in the study site will be associated with exceptionally dry periods in the overbank conditions. Gypsum, both inherited and pedogenic, is most abundant in soils under arid or semiarid climates as evaporative concentration is generally required for its formation (Poch, 2018). Gypsum crystals can develop in dry or ephemeral saline lake environments, where seasonal variations in groundwater level promote discontinuous growth of the crystals; these are interpreted as a record of variations of environmental conditions during gypsum growth (Mees et al., 2012; Poch et al 2018).

Accumulation of Fe and Mn were related to more humid periods, conditions of recent alluvial deposition with water table fluctuation or shallow water table. Decalcification and secondary carbonate accumulation require a seasonal climate with (semi) humid conditions providing excess rainfall and downward transport of seepage water (Ortiz et al., 2002). The presence of fine materials (silt – clay) and fine laminations is associated to calm deposition dynamics favoring the development of incipient A horizons; C horizons and low sorted deposits which were linked with more intense alluvial deposition dynamics in most humid weather conditions.

Despite the scarce pedogenetic development of these soils, it is possible to recognize different paleoclimatic periods and processes based on pedofeatures. From the taxonomic point of view, the first profile is classified as Fluvic Calcaric Loamic Oxyaquic Phaeozems, the second profile corresponds to a Gleyic Fluvic Cambic Calcaric Loamic Pyric Phaeozems (WRB, 2022). Fine-loamy Mixed Semiactive Calcareous Hyperthermic Torriorthentic Haplustolls (SSS, 2014).

4.3. Pedofeatures as paleoenvironmental indicators

The presence of septaric calcium carbonate nodules found on the study site is associated with more arid climatic conditions (very dry tropical forest) than the current ones. Cremaschi et al. (2015) report, on buried soils in alluvial sediments, the presence of carbonate leaching and slight hydromorphism as pedogenetical processes. The high content of charcoal in some horizons indicate the occurrence of fires. Regarding the presence of oriented and well-preserved charcoal fragments, they indicate short-distance transport conditions. The presence of rubefacted calcium carbonate nodules, fan-shaped micas due to dehydration, hornblendes broken in steps as a result of contraction, and the presence of abundant burned organic structures are associated with in situ burning conditions.

Vélez et al. (2013) report Early Holocene human activities in the area. Presence of finely comminuted charcoal, redistributed calcitic wood ash, dusty clay coatings and phosphatic aggregates records anthropogenic activities (Cremaschi et al., 2018). The composed juxtaposed pedofeatures were related to sequences of climatic changes. As a hypothesis is possible identify three climatically phases: phase I a dry climate stage (micrite hypo-

coatings), phase II with more humid conditions (iron oxide coatings and hypocoatings) indicating wetland under border alluvial environments and phase III a semiarid environment (gypsum crystals or sparite). The channels with dense complete infillings and crossed microlamination, as well as the presence of Fe oxide coatings show not very long periodic humid climate, since the charcoal and hornblende show little alteration. Preferred alignment of clay domains (stipple-speckled or granostriated b-fabric) and levels affected by carbonate precipitation (calcitic-crystallitic b-fabric), suggest alternating phases of pedogenic and sedimentary inputs (Zarate et al., 2000). The low pedogenetic development associated with scarce microstructural features, few root channels and the presence of mica sheets, were the product of fast rate of deposition.

The presence of olive and grey colors associated with root channels covered by iron oxides, show stagnic conditions (oxidoreductive environment), variations from dry to humid conditions which can be influenced by contrasting dry (Niño phenomena) and humid periods (Niña phenomena); or the geomorphological conditions that favor the accumulation of the water in the soil profile. Abundance of Fe coatings evidence long periods of water saturation, and abundance of Fe hypocoatings are related to intermittent saturation periods (Vepraskas et al., 2018). The Ab horizons present higher contents of organic matter, despite not observing accumulations of calcium carbonate in the morphological description, they have a high ionic content of Ca. Burnt vascular tissues, high content of organic remains, hypocoatings of Fe and Mn oxides were identified. The absence of soil features of carbonate accumulation in some layers, as well as the presence of coatings shown the occurrence of reducing environments; the higher content of organic matter was related to landscape stability and pedogenesis (phase II). The most recent phases of soil developed are mainly characterized by pedoturbation and calcite mobilization (Cremaschi et al., 2018). Redoximorphic features are associated with seasonal variation of the water table throughout the year under tropical dry forest conditions (phase I). The formation of concentric nodules occurs over multiple wet/dry cycles or fluctuations in the water table (Vepraskas et al., 2018). The presence of well-preserved organic remains evidences conditions of flooded soils quickly buried by deposition phenomena; the presence of abundant coprolites evidences a prolonged time of soil exposure without burial. Microlaminated coatings of illuvial clays and iron oxyhydroxides partially covered by lenticular gypsum crystals show dry environments, with a seasonal variation in soil moisture associated with the behavior of groundwater (phase III). The diatom remains identified in one of the horizons are characteristic of shallow inland waters (lacustrine), or saturated soils (Spaulding et al., 2010). This regime is subsequent to the deposition of the sediments, corresponds to conditions of small basins close to the channel.

The presence of non-laminated clay coatings with striated pattern, micrite coatings and hypo-coatings, and occasionally sparite coatings, low minerals weathering, Fe and Mn nodules and coatings, dense complete sand infillings and calcite coatings in channels evidence changes from humid climate (ferralization and mobilization of sand within the root channels) to dry climate (mobilization of carbonates) where polygonal structures

of calcium carbonate associated with plant remains are present. Ortiz et al. (2002), report discontinuous sedimentation and soil development governed by pulses of tectonic uplift, whereby the main pedogenic processes included leaching of carbonates and clay illuviation, the degree of development of horizons varied over time.

5. Conclusions

The results of the La Chorquina sediment sequence indicate that the parent material originated by successive deposition of alluvial fans on mountainous front formed by of the Guásimo landslide. The alluvial deposits in the study area were associated with several events of different causality, erosive events resulting from regional or local fires alternated with floods, and large-scale alluvial-torrential phenomena. Periods of relative stability were identified as responsible of the formation of incipient paleosols in relatively short time periods, under conditions of low weathering, which has allowed the preservation of the sedimentological characteristics of the deposit.

The deposits evidence environmental changes of great magnitude marked by three contrasting climatic periods, namely period III under semi-arid conditions (Tropical very dry forest), period I dry conditions (Tropical dry forest) to period II dry subhumid conditions. These changes in the climatic dynamics of the area may be related to changes in the ENSO dynamics. It is necessary to highlight that although the pedogenetic processes present in these soils are incipient, marked mostly by the dynamics of water associated with seasonal changes in precipitation, behavior of the water table and geomorphological position of the soil, it is nevertheless possible to identify seasonal paleoclimatic conditions through edaphological records in alluvial soils with little evolution, which makes these soils a tool for the study of Quaternary processes and paleoclimates in tropical fluvial environments.

References

Aceituno, F.J., Loaiza, N., 2015. The role of plants in the early human settlement of Northwest South America. Quaternary International 363, 20–27. https://doi.org/10.1016/j.quaint.2014.06.027

Benito, G., Rico, M., Díez Herrero, a., Sánchez-Moya, Y., Sopeńa, A., Thorndycraft, V.R., 2004. Hidrología de paleocrecidas y seguridad de presas. Riesgos Naturales y Entrópicos. [In:] Geomorfología. Actas de La VIII Reunión Nacional de Geomorfología. 89–98. (in Spanish)

Bradley, R.S., 1999. Paleoclimtology: Reconstructing Climates of the Quaternary. International Geophysics Series, 2d edition. Elsevier Academic Press, San Diego (USA), Vol. 68.

Bray, R.H, Kurtz, L.T., 1945. Determination of total, organic, and available forms of phosphorus in soil. Soil Science 59, 39-45. http://dx.doi.org/10.1097/00010694-194501000-00006

Buol, S.W., Southard, R.J., Graham, R.J., McDaniel, P.A., 2011. Soil Genesis and Classification, 6th Edition. Wiley-Blackwell, Oxford, UK, 527 p.

Castillo, N., 1988. Complejos arqueológicos y grupos étnicos del siglo XVI en el occidente de Antioquia. Boletín Museo Del Oro 0(20), 16–34. (in Spanish). website https://publicaciones.banrepcultural.org/index.php/bmo/article/view/7165

Cerón, W.L., Kayano, M.T., Ocampo, C., Canchala, T., Rivera, I., Avila, A., Andreoli, R.V., Parente de Souza, I., 2021. Spatio-Temporal Variability of Hydroclimatology in the Upper Cauca River Basin in Southwestern Colombia: Pre- and Post-Salvajina Dam Perspective. Atmosphere 12 1527. https:// doi.org/10.3390/atmos12111527

Colombo, F., 2010. Abanicos aluviales: secuencia y modelos de sedimentación. In Sedimentología: del proceso físico a la cuenca sedimentaria. Barcelona: Universidad de Barcelona, 131–224. (in Spanish)

Cremaschi, M., Zerboni, A., Nicosia, C., Negrino, F., Rodnight, H., Spötl, C., 2015. Age, soil-forming processes, and archaeology of the loess deposits at the Apennine margin of the Po Plain (northern Italy). New insights from the Ghiardo area. Quaternary International 376, 173-188. https://doi.org/10.1016/j.quaint.2014.07.044

Cremaschi, M., Trombino, L., Andrea, Z., 2018. Palaeosoils and Relict Soils: A Systematic Review. [In:] Stoops, G; Marcelino, V, Mees, F (Eds.). Interpretation of Micromorphological Features of Soils and Regoliths. Second Edition. 863–894. https://doi.org/10.1016/B978-0-444-63522-8.00029-2

Day, P.R., 1965. Particle fractionation and particle-size analysis. [In:] Black CA, (Eds.). Methods of soil analysis, part 1. Madison: American Society of Agronomy. 545–567.

Duchaufour, P., 1982. Pédologie. Tome I. Pédogenčse et Classification. Paris, Masson. 491 p.

Espinal, S., 1992. Geografía ecológica de Antioquia Zonas de Vida. Medellín: Universidad Nacional de Colombia, Sede Medellín. Lealon (Eds). Medellin – Colombia. (In Spanish)

García, Y.C., Martínez, J.I., Vélez, M.I., Yokoyama, Y., Battarbee, R.W., Suter, F.D., 2011. Palynofacies analysis of the late Holocene San Nicolás terrace of the Cauca paleolake and paleohydrology of northern South America – Palaeogeography, Palaeoclimatology, Palaeoecology 299 (1–2), 298–308. https://doi.org/10.1016/j.palaeo.2010.11.010

Gómez-Villar, A., 1996. Abanicos Aluviales: aportación teórica a sus aspectos más significativos. Cuaternario y Geomorfología 10(3–4), 77–124. (In Spanish).

González Iregui, H., 1976. Geología del cuadrángulo J-7, Informe 1704. Bogotá D.C. (In Spanish)

González Iregui, H., 1978. El Melange de Romeral y sus implicaciones tectónicas en la evolución de la cordillera Central, de los Andes Colombianos. II congreso Colombiano de Geología. Resúmenes. p14. (In Spanish)

González, H., 2001, Mapa Geológico del Departamento de Antioquia. Escala 1:400.000: Medellín, INGEOMINAS, 240 P. (in Spanish) https://recordcenter.sgc.gov.co/B4/13010040024267/documento/pdf/0101242671101000.pdf

Grosse, E., 1926. El Terciario Carbonífero de Antioquia. Reimer, D., Vohsen, E. (Eds.), Berlín. 342p. (In Spanish and German) https://www.accefyn.com/cientificos/pdf/emilGrosse/EmilGrosse.pdf

Harvey, A.M., 2002. The role of base-level change in the dissection of alluvial fans: Case studies from southeast Spain and Nevada. Geomorphology 45(1–2), 67–87. https://doi.org/10.1016/S0169-555X(01)00190-8

IUSS Working Group WRB, 2022. World Reference Base for Soil Resources. International soil classification system for naming soils and creating legends for soil maps. 4th edition. IUSS Working Group WRB. International Union of Soil Sciences (IUSS), Vienna, Austria. 234 p.

Johnstone, D., 2014. Geomorphology, paleopedology and sedimentology of the Holocene sediments of the Santa Fe – Sopetrán Basin, Antioquia Colombia. Unpublished Msc Thesis University of Regina. Canada.

Kumar, R., Suresh, N., Sangode, S. J., Kumaravel, V., 2007. Evolution of the Quaternary alluvial fan system in the Himalayan foreland basin: Implications for tectonic and climatic decoupling. Quaternary International 159(1), 6–20. https://doi.org/10.1016/j.quaint.2006.08.010

Loaiza-Usuga, J.C., Poch, R.M., 2015. Muestreo de suelos con énfasis en micromorfología. [In:] Loaiza, J.C., Stoops, G., Poch, R.M., Casamitjana, M. (Eds.), Manual de Micromorfología de suelos y técnicas complementarias. Fondo Editorial Pascual Bravo. Medellín – Colombia. (In Spanish)

Loaiza-Usuga, J.C., Stoops, G., Poch R.M., Casamitjana, M., 2015. Manual de micromorfología de suelos y técnicas complementarias. Fondo Editorial Pascual Bravo. Medellín – Colombia. 384 pp. (In Spanish)

Martínez, J.I., Mayr, C., Yokoyama, Y., Vélez, M.I., Battarbee, R., 2013. The San Nicolás succession of the Cauca paleolake: A late Holocene laminated ria lake record from the Neotropics. Journal of Paleolimnology 49. https://doi.org/10.1007/s10933-012-9676-4

Martínez, J.I., Obrochta, S., Yokoyama, Y., Battarbee, R.W., 2015. Atlantic Multidecadal Oscillation (AMO) forcing on the late Holocene Cauca paleolake dynamics, northern Andes of Colombia. Climate of the Past Discussions 11, 2649–2664. https://doi.org/10.5194/cpd-11-2649-2015

Martinez-Sacristan, H., 2017. Landslides in Colombia: Could Similar Incidents Happen Again?. [In:] M, Ibaraki., Mori, H. (Eds), Progress in Medical Geology. Cambridge Schoolars publishers.p 232.

Mees, F., Castañeda, C., Herrero, J., Van Ranst, E., 2012. The nature and significance of variations in gypsum crystal morphology in dry lake basins. Journal of Sedimentary Research 82, 41–56. https://doi.org/10.2110/jsr.2012.3

Mesa, M.I., 2003. Propuesta de una Metodología Cuantitativa para Identificar Ritmitas en un Depósito Lacustre del río Cauca, Santa Fe de Antioquia. MSc Thesis, Universidad Nacional de Colombia, Sede Medellín. (In Spanish)

Nickel, E., 1985. Carbonates in alluvial fan systems. An approach to physiography, sedimentology and diagenesis. Sedimentary Geology 42 (1–2), 83–104. https://doi.org/10.1016/0037-0738(85)90075-2

Olivera, D., Tchilinguirian, P., Grana, L., 2004. Paleoambiente y arqueología en la Puna meridional argentina: archivos ambientales, escalas de análisis y registro arqueológico. Relaciones de La Sociedad Argentina de Antropología XXIX, 229–247. (In Spanish)

Ortiz, E.A., Pérez, Y., 1998. Características geológicas y geomorfológicas del mega deslizamiento del Guásimo. Master Thesis, Universidad Nacional de Colombia, Sede Medellín. (In Spanish with English abstract)

Ortiz, I., Simón, M., Dorronsoro, C., Martín, F., García, I., 2002. Soil evolution over the Quaternary period in a Mediterranean climate (SE Spain). Catena 48, 131–148. https://doi.org/10.1016/S0341-8162(01)00194-1

Page, W.D., Mattsson, L., 1981. Landslide lakes near Santa Fe de Antioquia. Revista CIAF – 6, 469–478. (In Spanish)

Paris, G., Machette, M.N., Dart, R.L., Haller, K.M., 2000. Map and Database of Quaternary Faults and Folds in Colombia and its Offshore Regions. Open – File Report 00-0284. Denver, Colorado, USA. https://pubs.usgs.gov/of/2000/ofr-00-0284/ofr-00-0284.pdf

Parra-Sánchez, L.N., 1997. El Terciario del valle del Río Cauca al Norte de la Barrera de Cangrejo -Borde Oeste. Universidad Nacional de Colombia, Sede Medellín, Unpublished data. (In Spanish)

Poch, R.M., Artieda, O., Herrero, J., Lebedeva-Verba, M., 2028. Gypsic Features. [In:] Stoops, G., Marcelino, V., Mees, F. (Eds.), Interpretation of Micromorphological Features of Soils and Regoliths, Second edition. Elsevier. 195–216. https://doi.org/10.1016/B978-0-444-53156-8.00010-6

Porta Casanellas, J., 1986. Técnicas y Experimentos en Edafología. Colegio Oficial de Ingenieros Agrónomos de Catalunya, Barcelona. (In Spanish)

Poveda, G., Waylen, P.R., Pulwarty, R.S., 2006. Annual and inter-annual variability of the present climate in northern South America and southern Mesoamerica. Palaeogeography, Palaeoclimatology, Palaeoecology 234(1), 3–27. https://doi.org/10.1016/j.palaeo.2005.10.031

Rodríguez, G., Arango, M.I., 2013. Formación Barroso: Arco Volcánico Toleitico Y Diabasas De San José De Urama: Un Prisma Accrecionario T-Morb En El Segmento Norte De La Cordillera Occidental De Colombia. Boletín Ciencias de La Tierra 33, 17–38. https://doi.org/ISSN 0120-3630

Serna, Y., Vélez, M.I., Escobar, J., 2015. Microscopic organic matter particles in late Holocene riparian sediments near the Cauca River, Colombia. Journal of Paleolimnology 54(4), 325–344. https://doi.org/10.1007/s10933-015-9855-1

Shukla, U.K., Singh, I.B., Sharma, M., Sharma, S., 2001. A model of alluvial megafan sedimentation: Ganga Megafan. Sedimentary Geology 144(3–4), 243–262. https://doi.org/10.1016/S0037-0738(01)00060-4

Silva–Tamayo, J.C., Lara, M., Salazar–Franco, A.M., 2020. Oligocene – Miocene coal–bearing successions of the Amagá Formation, Antioquia, Colombia: Sedimentary environments, stratigraphy, and tectonic implications. In: Gómez, J. & Mateus–Zabala, D. (editors), The Geology of Colombia, Volume 3 Paleogene – Neogene. Servicio Geológico Colombiano, Publicaciones Geológicas Especiales 37, 23 p. Bogotá. (in Spanish) https://doi.org/10.32685/pub.esp.37.2019.11

SSS, 2004. Soil survey laboratory methods manual. [In:] Burt, R (Ed). USDA-NRCS Gov't Printing Office. Washington D.C.

SSS, 2014. Keys to soil taxonomy. 12th ed. United States Department of Agriculture (USDA). Natural Resources Conservation Service (NRCS). 372p.

SSS, 2018. Soil survey manual. Tech. Rep. No 18. Washington, DC: Soil Survey Division Staff, Soil Conservation Service, US Department of Agriculture. 603 p.

Spaulding, S.A., Lubinski, D.J., Potapova, M., 2010. Diatoms United States: Diatom identification guide and ecological resource. Web-based resource. https://www.researchgate.net/publication/256115780_Diatoms_of_the_United_States_Web-based_resource

Stoops, G., 2021. Guidelines for Analysis and Description of Soil and Regolith Thin Sections. Second Edition. John Wiley & Sons, Inc. Madison. USA. 248p.

Suter, F., Martínez, J.I., 2009. Tectónica transpresiva cuaternaria en la sutura de El Romeral: ejemplo de la cuenca de Santa Fé-Sopetrán, Antioquia. XII Colombian Geol. Congr. Paipa, Colombia. (In Spanish).

Suter, F., Martínez, J.I., Vélez, M.I., 2011. Holocene soft-sediment deformation of the Santa Fe-Sopetrán Basin, northern Colombian Andes: Evidence for pre-Hispanic seismic activity? Sedimentary Geology 235(3–4), 188–199. https://doi.org/10.1016/j.sedgeo.2010.09.018

Suter, F., Sartori, M., Neuwerth, R., Gorin, G., 2008. Structural imprints at the front of the Chocó-Panamá indenter: Field data from the North Cauca Valley Basin, Central Colombia. Tectonophysics 460 (1–4), 134–157. https://doi.org/10.1016/j.tecto.2008.07.015

Tauler, E., Canals, A., 2015. Mineralogía óptica. [In:] Loaiza, J.C., Stoops, G., Poch, R.M., Casamitjana, M. (Eds.), Manual de Micromorfología de suelos y técnicas complementarias. Fondo Editorial Pascual Bravo. Medellín – Colombia. (In Spanish)

Valencia, J.M., García, C.E., Montero, D., 2017. Vegetation anomalies associated with the ENSO phenomenon in the Cauca river valley, Colombia – Revista de Teledetección 50, 89–99. (In Spanish with English abstract) https://doi.org/10.4995/raet.2017.7715

Vélez, M.V., Rhenals, R.L., 2008. Determinación de la Recarga con Isótopos Ambientales en los Acuíferos de Santa Fe de Antioquia. Boletín de Ciencias de La Tierra 24, 37–54. (In spanish with English abstract)

Vélez, M.I., Martinez, J.I., Suter, F., 2011. Late Holocene history of the floodplain lakes of the Cauca River, Colombia. Journal of Paleolimnology 49(4), 591–604. https://doi.org/0.1007/s10933-012-9663-9

Vepraskas, M.J., Lindbo, D.L., Stolt, M.H., 2018. Redoximorphic Features. [In:] Stoops, G; Marcelino, V., Mees, F. (Eds.), Interpretation of Mi-

cromorphological Features of Soils and Regoliths. Second Edition. 425–445. https://doi.org/10.1016/B978-0-444-63522-8.00015-2

Vinasco, C., Cordani, U., 2012. Reactivation episodes of the Romeral Fault System in the northwestern part of Central Andes, Colombia, through 39Ar-40Ar and K-Ar results. Boletín Ciencias de la Tierra 32. 111–124. http://www.scielo.org.co/pdf/bcdt/n32/n32a10.pdf

Viseras, C., Calvache, M.L., Soria, J.M., Fernández, J., 2003. Differential features of alluvial fans controlled by tectonics or eustatic accommodation space. Examples from the Betic Cordillera, Spain. Geomorphology 50(1–3), 181–202. https://doi.org/10.1016/S0169-555X(02)00214-3

Walkley, A., Black, A., 1934. An examination of Degtjareff method for determining soil organic matter and a proposed modification of the chromic acid titration method. Soil Science 37, 29-37.

Weber, M., Gómez-Tapias, J., Cardona, A., Duarte, E., Pardo-Trujillo, A., Valencia, V.A., 2015. Geochemistry of the Santa Fe Batholith and Buriticá Tonalite in NW Colombia – Evidence of subduction initiation beneath the Colombian Caribbean Plateau – Journal of South American Earth Sciences 62, 257–274. https://doi.org/10.1016/j.jsames.2015.04.002

Weber, M., Gómez-Tapias, J., Duarte, E., Cardona, A., Vinasco-Vallejo, C.J., 2011. Geochemistry of the Santa Fe Batholith in NW Colombia: Remnant of an Accreted Cretaceous Arc. Memorias XIV Congreso Latinoamericano de Geología. Medellín, Colombia. 128–129.

Zárate, M., Kemp, R.A., Espinosa, M., Ferrero, L., 2000. Pedosedimentary and palaeoenvironmental significance of a Holocene alluvial sequence in the southern Pampas, Argentina. The Holocene 10, 481–488. https://doi.org/10.1191/095968300669846317